Pharm Res (2013) 30:2133–2145
DOI 10.1007/s11095-013-1071-y

RESEARCH PAPER

Effects of Cerium Oxide Nanoparticles on PC12 Neuronal-Like Cells: Proliferation, Differentiation, and Dopamine Secretion

Gianni Ciofani • Giada G. Genchi • Ioannis Liakos • Valentina Cappello • Mauro Gemmi • Athanassia Athanassiou • Barbara Mazzolai • Virgilio Mattoli

Received: 7 February 2013 / Accepted: 3 May 2013 / Published online: 10 May 2013

ABSTRACT

Purpose Oxidative stress has been found to play a key role in several diseases, that range from cancer to neurodegenerative disorders. Besides traditional anti-oxidant agents, in recent years much attention has been focused on nanotechnological solutions, including cerium oxide nanoparticles (nanoceria).

Methods Thanks to its extraordinary catalytic properties, nanoceria mimics the activity of superoxide dismutase and of catalase, therefore acting as a reactive oxygen species (ROS) scavenger in many biological contexts. In this paper, we report on nanoceria interactions with PC12 cell line, that represents a valuable model for many features of central dopaminergic neurons.

Results Nanoceria confirmed a strong anti-ROS action but, most interestingly, also showed beneficial effects on both cell differentiation and dopamine production.

Conclusions Even if deeper examinations will be necessary in order to better clarify the mechanisms at the base of the documented effects, nanoceria demonstrated a significant potential as pharmacological agent in the treatment of neurological disorders.

G. Ciofani (✉) • G. G. Genchi • B. Mazzolai • V. Mattoli
Istituto Italiano di Tecnologia, Center for Micro-BioRobotics @SSSA
Viale Rinaldo Piaggio 34
56025 Pontedera, Pisa, Italy
e-mail: gianni.ciofani@iit.it

G. G. Genchi
Scuola Superiore Sant'Anna, The BioRobotics Institute
Viale Rinaldo Piaggio 34
56025 Pontedera, Pisa, Italy

I. Liakos • A. Athanassiou
Istituto Italiano di Tecnologia
Center for Biomolecular Nanotechnologies @UniLe, Via Barsanti
73010 Arnesano, Lecce, Italy

V. Cappello • M. Gemmi
Istituto Italiano di Tecnologia, Center for Nanotechnology Innovation
@NEST, Piazza San Silvestro 12
56127 Pisa, Italy

KEY WORDS cerium oxide nanoparticles · dopamine · PC12 cells · reactive oxygen species production scavenger

ABBREVIATIONS

EDS	energy-dispersive X-ray spectroscopy
ELISA	enzyme-linked immunosorbent Assay
NC	nanoceria
NGF	nerve growth factor
ROS	reactive oxygen species
XPS	X-ray photoelectron spectroscopy

INTRODUCTION

Cerium oxide nanoparticles (nanoceria, NC) represent an extremely interesting class of nanomaterials that, thanks to its intriguing catalytic activity (1), found plenty of applications in several fields, that range from solid oxide fuel cells to gas sensors (2).

CeO_2 presents a fraction of Ce in the Ce^{3+} form compensated by an analogous number of oxygen vacancies. This phenomenon is enhanced at the nanoscale level because of the higher surface/volume ratio, and implies the coexistence of Ce^{3+} and Ce^{4+} ions, that are involved in redox reactions (3). In a biological context, it has been shown that NC is able to scavenge reactive oxygen species (ROS), mimicking both the activity of superoxide dismutase (the enzyme that catalyzes the dismutation of the superoxide radical anion), and of catalase (the enzyme that decomposes H_2O_2 to O_2 and H_2O) (4,5).

The use of NC as a free-radical scavenger has therefore become popular for biological applications: NC was in fact proven to be an extremely efficient protective agent for cardiac (6), neuronal (7), and stem (8) cells. Moreover, *in vivo*, NC confirmed to show strong anti-oxidative properties in mice (9), to prevent loss of retinal function

in rats (10,11), to promote the regression of pathologic retinal neovascularization in mice (12), and to promote wound healing activity (13). A comprehensive review on potential pharmacological applications of NC is represented by the work of Celardo and collaborators (14), to which readers are referred.

The huge interest in antioxidant effects of NC stems for the essential role of ROS in the development of several diseases, when they are not adequately buffered by the natural antioxidant defenses of the cells. It has indeed been proven, that ROS (like superoxide anion radical $O_2^{\bullet -}$, hydroxyl radical $OH^{\bullet -}$, singlet oxygen $^1O_2$, and hydrogen peroxide H_2O_2) are extremely reactive chemical species that play a key role in cancer (15), neurodegenerative disorders (16), inflammation (17), and in many other pathological conditions (18). In particular, ROS are able to oxidize many biological macromolecules, affecting in particular the hydrocarbon chains of unsaturated fatty acids, aminoacid residues in proteins, carbohydrates, and nitrogenous bases in nucleic acids. This oxidation compromises structure and function of the biological macromolecules, often resulting in cell death (19).

Concerning neurological applications, NC has been very recently proposed for the treatment of neurological diseases (20), such as Alzheimer's, Parkinson's, and Gehrig's. As an example, Cimini *et al.* proposed polyethylene glycol (PEG)-coated and antibody-conjugated NC for the selective targeting of amyloid-β 1–42 aggregates, that are the main responsible of Alzheimer's disease, showing an improvement of neuronal survival, by modulating the brain-derived neurotrophic factor (BDNF) signaling pathway (21).

Another study showed the neuroprotective mechanisms of NC in a model of ischemia (22). The neuroprotective effects resulted due to a modest reduction in reactive oxygen species, and, more significantly, to a strong decrement of the levels of ischemia-induced 3-nitrotyrosine, a modification of tyrosine residues in proteins induced by the peroxynitrite radical.

In this paper, we report on the effects of incubation of PC12 neuron-like cells with increasing concentrations of a commercial NC. After an extensive characterization of the nanomaterial, we evaluated viability, proliferation and differentiation of the cells in the presence of CeO_2 nanoparticles. No evidences of toxicity were found; instead, an increment of differentiation in terms of neurite length was found when cells underwent treatment with NC. ROS production evaluation confirmed anti-oxidant properties of NC also in this kind of cells. Finally, and most interestingly, we analyzed the effects of NC on dopamine production, that is impaired in Parkinson's disease, showing beneficial effects of nanoparticles in dopamine secretion. Effects of NC on PC12 cells were also investigated at gene level. All these results corroborate the need of further investigations of NC as a therapeutic agent, suggesting special attention to neurodegenerative processes.

MATERIALS AND METHODS

Nanoparticle Characterization

Cerium oxide nanoparticles (nanoceria, NC) were purchased by Sigma (code 544841) and underwent extensive characterization before biological testing.

Transmission electron microscopy was performed on a Zeiss Libra 120 operating at 120 kV. The samples were prepared by deposition of CeO_2 nanoparticles in physiologic saline solution (0.9% NaCl in H_2O) on a 300 mesh carbon coated copper grid.

Energy-dispersive X-ray spectroscopy (EDS) microanalysis was performed using a scanning electron microscope (SEM, EVO MA10 Zeiss) with NC deposited on silicon wafers and gold-sputtered before analysis.

Cerium nanoparticles were characterized through X-ray photoelectron spectroscopy (XPS) in order to qualitatively and quantitatively assess Ce^{3+} and Ce^{4+} content. XPS measurements were performed using a Specs Lab2 electron spectrometer equipped with a monochromatic X-ray source (set at 1,253 eV) and with a Phoibos analyzer Has 3500 (Emispherical Energy Analyzer). The applied voltage of the Mg Kα X-ray source was set at 13 kV and the applied current at 15 mA. The pressure in the analysis chamber was approximately $7 \cdot 10^{-9}$ mbar. For Ce $3d_{5/2}$ and Ce $3d_{3/2}$ spectra acquisition, the energy pass was 30 eV, the energy step 0.2 eV and the scan number 40. The spectra were then analyzed using CasaXPS software.

Nanoparticles were mixed with the appropriate culture medium at a concentration of 1 mg/ml and sonicated for 2 h (with a Bransonic sonicator 2510) using an output power of 20 W, just before their administration to cell cultures. The obtained dispersion was then diluted at fixed concentrations (see next sections for details) for biological experiments. For EDS analyses, nanoparticles were dispersed in distilled water using the same procedure.

Particle size distribution and Z-potential of the dispersions were analyzed with a Nano Z-Sizer 90 (Malvern Instrument). For both analyses, each acquisition was performed three times, using samples appropriately diluted in complete cell culture medium.

Cell Culture and Viability Assays

PC12 cells (ATCC CRL-1721) are derived from a transplantable rat pheochromocytoma, and represent a valuable

model for neuronal differentiation, mimicking many features of central dopaminergic neurons, including dopamine production. Moreover, they can reversibly respond to the administration of nerve growth factor (NGF), expressing sympathetic neuronal phenotype (23). PC12 were cultured in Dulbecco's modified Eagle medium (DMEM) with 10% horse serum (HS), 5% fetal bovine serum (FBS), 100 IU/ml penicillin, 100 μg/ml streptomycin and 2 mM L-glutamine. Differentiation was induced by administration of a low-serum (1% FBS) medium supplemented with 50 ng/ml of NGF.

For viability testing, PC12 cells were seeded in 96-well plates (5,000 cells *per* well) and incubated with increasing concentrations of NC (0, 10, 20, 50 and 100 μg/ml). At 24 and 72 h since beginning of treatment, cell metabolism was assessed with the WST-1 assay (2-(4-iodophenyl)-3-(4-nitophenyl)-5-(2,4-disulfophenyl)-2H-tetrazoilium monosodium salt, provided in a pre-mix electro-coupling solution, BioVision). Cell cultures were treated with 100 μl of culture medium added with 10 μl of the pre-mix solution for 2 h and, finally, absorbance was read at 450 nm with a microplate reader (Victor3, Perkin Elmer).

Viability was further qualitatively investigated at 72 h with the Live/Dead® viability/cytotoxicity Kit (Molecular Probes). The kit contains calcein AM (4 mM in anhydrous DMSO) and ethidium homodimer-1 (EthD-1, 2 mM in DMSO/H_2O 1:4 (v/v)), and allows for the discrimination between live cells (stained in green by calcein) and dead cells (stained in red by EthD-1). Cultures were rinsed with PBS, treated for 10 min at 37°C with 2 μM calcein AM and 4 μM EthD-1 in PBS, and finally observed with an inverted fluorescence microscope (TE2000U, Nikon) equipped with a cooled CCD camera (DS-5MC USB2, Nikon) and with NIS Elements imaging software.

Differentiation capability in the presence of NC was evaluated providing cell cultures (30,000 cells in 24-well plates) with differentiating medium doped with 0, 20 and 50 μg/ml of NC. After 3 days, differentiating status was assessed through immunofluorescence analysis of specific neuronal differentiation markers, β3-tubulin and neurofilament-66, followed by ImageJ analysis (http://rsb.info.nih.gov/ij/) of the neurite length (at least 100 neurites *per* sample were measured for statistical analysis purpose).

Samples were rinsed with PBS and fixed in paraformaldehyde (4% in PBS) for 15 min. After rinsing with PBS, they were incubated with sodium borohydryde (1 mg/ml in PBS) for 10 min to reduce autofluorescence. Cellular membranes were then permeabilized with 0.1% Triton X-100 in PBS for 15 min. Antibody aspecific binding sites were saturated with 10% goat serum in PBS for 1 h, and, subsequently, a primary antibody (rabbit polyclonal IgG anti-tubulin, Sigma, diluted 1:75 in 10% goat serum, or rabbit monoclonal IgG anti-neurofilmanent, Millipore, diluted 1:250 in 10% goat serum) was added. After 30 min of incubation at 37°C, samples were rinsed with 10% goat serum; then, a staining solution was added, composed of a secondary antibody (fluorescent goat anti-rabbit IgG, Invitrogen) diluted 1:250 in 10% goat serum and of 1 μM DAPI for nucleus counterstaining. After 30 min of incubation at room temperature, samples were rinsed with 0.45 M NaCl in PBS for 1 min to remove weakly bound antibodies and, after rinsing in PBS, observed with the inverted fluorescence microscope.

ROS Production Assessment

Intracellular ROS production was induced in cells cultured in 24-well plates (30,000 cells *per* well) by a 50 μM H_2O_2 treatment of 30 min in complete medium, after being exposed for 72 h to 0, 20, and 50 μg/ml of NC. Controls on cells non-treated with H_2O_2 were also performed. ROS production was quantified with the 20,70-dichlorfluorescein diacetate (DCFH-DA) test. DCFH-DA is a membrane-permeant compound that, once inside cells, is deacetylated by endogenous esterases to form the non-fluorescent 20,70-dichlorfluorescein (DCFH). DCFH is thereafter converted to green fluorescent dichlorofluorescein (DCF) compound by the action of cellular oxidants. Following ROS production, green fluorescence is therefore emitted by the cells. After H_2O_2 treatment, cells were incubated with 50 μM DCFH-DA in DMEM without serum for 30 min at 37°C and then observed at the fluorescence microscope or lysed though three freezing/thawing cycles to quantitatively assess fluorescence through the microplate reader (excitation wavelength 485 nm, emission wavelength 535 nm).

Dopamine Secretion Assessment

Dopamine production was quantified collecting supernatants after 72 h of incubation of proliferating cells with 0, 20, and 50 μg/ml of NC (30,000 cells *per* well, in 24-plate wells). A solid phase Enzyme-Linked Immunosorbent Assay (ELISA), based on the sandwich principle, was carried out with a Dopamine ELISA kit (GenWay Biotech Inc.), following the manufacturer's instructions. Briefly, 20 μl of extracted samples were incubated for 2 h at room temperature in wells coated with a goat anti-rabbit antibody, directed towards a dopamine epitope. An enzyme-conjugated secondary antibody, directed towards a different region of the dopamine molecule, was thus added and incubated at room temperature for 1 h. Appropriate substrate was thereafter provided to the enzyme-conjugated antibody and reaction was allowed to occur for 40 min at room temperature. Absorbance of the colored product was finally measured at 405 nm on the microplate reader and compared to a calibration curve (obtained with known amounts

of dopamine) for neurotransmitter concentration determination. Obtained values were normalized to the cell number, evaluated by measuring total DNA content with the PicoGreen® kit (Molecular Probes) following the manufacturer's instruction. After cell lysis, the PicoGreen® dye binds to ds-DNA and the resulting fluorescence intensity is directly proportional to the ds-DNA concentration in solution and, therefore, to the cell number. Fluorescence intensity was measured with the microplate reader using an excitation wavelength of 485 nm and an emission wavelength of 535 nm.

Quantitative RT-PCR

Transcription of specific genes of markers of neuronal cell maturation (neurofilament-66, *Nefl*, and β3-tubulin, *Tub*), of ROS mechanisms (glutathione peroxidase 1, *Gpx1*; glutathione synthetase, *Gss*; thioredoxin reductase-1, *Txnrd1*), of dopamine metabolism (tyrosine hydroxylase, *Th*; monoamine oxidase A, *Maoa*; catechol-O-methyltransferase, *Comt*), and of dopamine transport (dopamine transporter, *Dat*; vesicular monoamine transporter-2, *Vmat2*) were evaluated with quantitative real-time qRT-PCR at 3 days of incubation with 0, 20, and 50 μg/ml of NC. Total RNA was isolated from cell cultures using High Pure RNA Isolation kit (Roche) according to the manufacturer's protocol. Extracted RNA was diluted ten times in pure water (MilliQ Millipore) and RNA concentration was measured at 260 nm with a spectrophotometer (Lambda 45, Perkin Elmer). RNA retrotranscription into cDNA was performed with 400 ng of RNA in a total volume of 20 μl, including 4 μl of iScriptTM Reverse Transcription Supermix (5X, Bio-Rad). The synthesis program included an initial incubation at 25°C for 5 min, followed by incubation at 42°C for 45 min and at 48°C for 15 min. Reaction was inactivated by heating at 85°C for 5 min, and the reaction volume was finally increased up to 200 μl with pure water.

Quantitative RT-PCR was performed with a CFX Connect™ Real-Time PCR Detection System (Bio-Rad) to determine the transcription of different genes. Results were normalized to the transcription levels of a selected housekeeping gene, glyceraldehyde 3-phosphate dehydrogenase (*Gapdh*). The obtained cDNA (5 μl) was mixed with 1 μl of specific forward and reverse primers (8 μM), 4 μl of MilliQ and 10 μl of SsoAdvancedTM SYBR®Green Supermix (Bio-rad). The thermal protocol was applied with one cycle of 30 s at 98°C for enzyme activation, followed by 40 cycles at 98°C for 3 s and 60°C for 7 s. After the last reaction cycle, the protocol included a temperature ramp from 65°C to 95°C, with 0.5°C/s increments, to exclude unspecific products with melting curve results. Each assay included "no template" sample and all tests were carried out in triplicate. The cycle threshold (Ct) value relative of control sample was adopted as reference for the calculation of ΔΔCt (difference between ΔCt values deriving from difference between Ct of target and housekeeping gene) for the subsequent samples. Primer sequences (forward and reverse) of the investigated genes are reported in Table I.

Statistical Analysis

Analysis of the data was performed by analysis of variance (ANOVA) followed by Tukey's post-test to test for significance, which was set at 5%. Results are presented as mean value ± standard deviation ($n=6$ for the WST-1 assays, $n=3$ for all other analysis).

RESULTS

NC Characterization

Transmission electron microscopy shows that the CeO_2 nanoparticles are quite dispersed in size, in a range going from 5 nm to 80 nm. Powder electron diffraction patterns taken on areas of 10 μm in diameter, that are rich of nanoparticles, show sharp diffraction rings indicating that the nanoparticles have a crystalline nature. The patterns can be indexed with a cubic face centered lattice. A Le Bail fit

Table I Primer Sequences for qRT-PCR Analysis

Gene	Sequence
Gapdh	5′-AACCTGCCAAGTATGATGAC-3′
	5′-GGAGTTGCTGTTGAAGTCA-3′
Nefl	5′-GAGAAGCAGAAGAGGAGGAG-3′
	5′-TGGCATCTTCAGACTCATCC-3′
Tub	5′-ATTCTGGTGGACCTGGAG-3′
	5′-CACTCTGACCGAAGATAAAGTT-3′
Gpx1	5′-CATTGTTTGAGAAGTGCGAGGTG-3′
	5′-ACTGGGTGCTGGCAAGGC-3′
Gss	5′-CCAGCGTGCCATAGAGAAC-3′
	5′-CCCTTTCAGAGACATCTTCAAATC-3′
Txnrd1	5′-TGGAAGAGCATGGTATCAAG-3′
	5′-CACGGTCTCTAAGCCAATAG-3′
Th	5′-CTGTTCTCAACCTGCTCTTC-3′
	5′-TGGCTTCAAATGTCTCAAATAC-3′
Maoa	5′-CAGACACACCAGACAACAC-3′
	5′-TACGGACATAGGCACTGAG-3′
Comt	5′-CCTGACTTCCTGGCGTATG-3′
	5′-TTCTCCAAGCCGTCTACAAC-3′
Dat	5′-TGGACTTCTACCGACTCTG-3′
	5′-GGAGGTGGTGATGATTGC-3′
Vmat2	5′-AGCATCTTCTCTTACTATAACAAC-3′
	5′-AAACAGCAGCCCAACTTG-3′

(24) of the integrated pattern gives a unit cell parameter of $a = 5.402 \pm 0.005$ Å which is compatible with that one of CeO_2 cubic ceria.

EDS analysis (Fig. 1b) performed on the sample confirmed its high purity, being composed by Ce ~30% and O ~65% (atom content). A small amount of gold, deriving from the sputtering procedure, is also present (~4%); impurities were found to be less of the 1% of atom content.

Since oxidation state is a key component of NC catalytic activity, it is mandatory to assess the presence of adequate amounts of Ce^{3+} and Ce^{4+} on the nanoparticle surface. Figure 1c shows the Ce $3d_{5/2}$ and Ce $3d_{3/2}$ XPS spectra and the related Gaussian peak deconvolution acquired from the NC powder. The peaks in the range 875–895 eV belong to the Ce $3d_{5/2}$, while the peaks in the range 895–910 eV correspond to the Ce $3d_{3/2}$ levels. Basing on the shift reported in the literature (25), we could assign peaks at

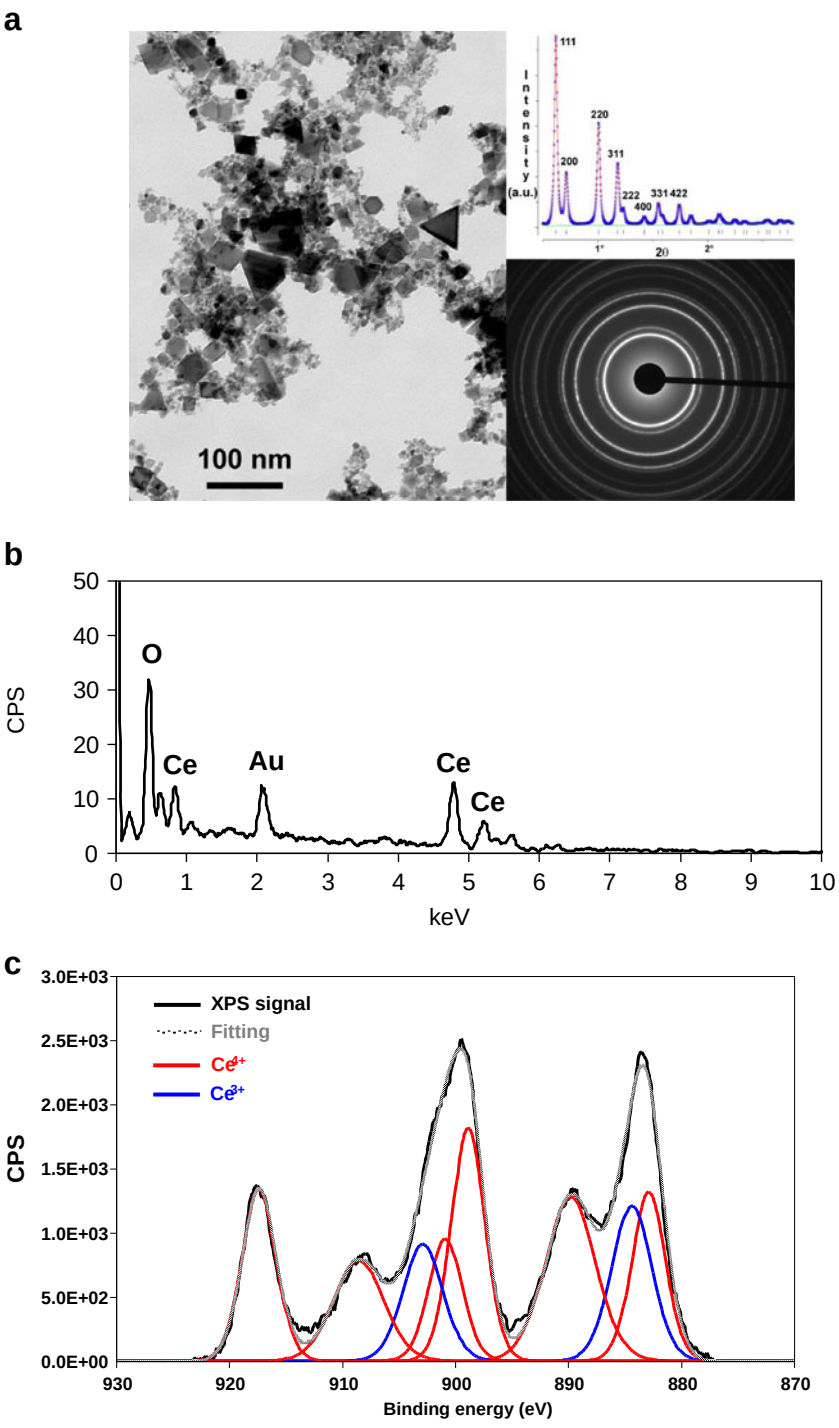

Fig. 1 Cerium oxide nanoparticle characterization: TEM bright field imaging (*left*), powder electron diffraction pattern (*bottom right*), radially integrated profile of the pattern fitted with the Le Bail method (*top right*) with the positions and the indices of the diffracted peaks (**a**); EDS analysis (**b**) and high resolution XPS analysis of Ce $3d_{5/2}$ and Ce $3d_{3/2}$ (**c**).

882.9, 889.8, 900.9, 908.6 and at 917.4 eV to Ce^{4+}, while peaks at 884.4 and 902.9 eV to Ce^{3+}. From the ratio of the integrated peak areas, we can deduce a Ce^{3+} content of ~23%, that has been demonstrated to be optimal for NC redox activity (26).

In order to characterize NC assembling in cell culture medium and to have a hint of the actual sizes of the nanocomplexes in the cultures, dynamic light scattering (DLS) and Z-potential analyses were performed in complete cell culture medium. DLS revealed a 92.0% peak at a size of about 230 nm, with a polydispersity index of 0.290. Moreover, a Z-potential of about −15 mV (deriving from an absorption of serum proteins on the nanoparticles) denoted a good stability of the obtained dispersion.

PC12 Cells Viability and Differentiation in the Presence of NC

WST-1 provided an excellent metabolic activity in cells treated up to 100 μg/ml of NC (Fig. 2a), with no statistically significant decrement of viability, at all the tested concentrations, after both 24 and 72 h.

Viability was further investigated with the Live/Dead® viability/cytotoxicity Kit. Also in this case, the compatibility of NC resulted optimal at each concentration (Fig. 2b) after 72 h of incubation. No evidence of cell membrane damage was present following treatment of cells up to 100 μg/ml of NC, clearly demonstrating a viability comparable to that of the control cultures (less than 1% of red, *i.e.*, necrotic, cells).

PC12 cells retained differentiation capability in the presence of NC, as depicted in Fig. 3. After 3 days since differentiation induction, PC12 cells exhibited a well-developed neurite network, with a strong expression of typical neuronal marker such as β3-tubulin and neurofilament-66, as suggested by the intense fluorescence signal of the images.

Interestingly, a quantitative analysis carried out on neurite length showed a beneficial effect of NC on neuronal differentiation. Figures 4a–c depict length distribution of neurites of cells treated with 0, 20 and 50 μg/ml of NC during the 3-day differentiation. Control cultures exhibit a median neurite length value of about 55 μm (min 25 μm, average 60 μm, max 175 μm), that increases to about 65 μm (min 30 μm, average 70 μm, max 140 μm) in the case of cells treated with 20 μg/ml of NC, and up to 85 μm (min 35 μm, average 90 μm, max 180 μm) when the concentration of NC was 50 μg/ml.

An improved differentiation was confirmed by analysis at gene level with qRT-PCR (Fig. 4d). In this case, a slight, but statistically significant increment ($p<0.05$) of gene transcription is appreciable just in cells treated with 50 μg/ml of NC, that show a 1.5 fold increment of both β3-tubulin and neurofilament-66 genes.

NC as ROS Scavenger in PC12 Cells

Intracellular antioxidant activity of nanoceria was tested both on cultures stimulated and non-stimulated with H_2O_2. Figure 5a shows fluorescence images of cells stimulated with H_2O_2 for 30 min after a 3-days incubation with NC. It can be clearly seen that NC reduces production of ROS in cells in a dose-dependent manner.

This result is confirmed by a quantitative evaluation of the fluorescence due to DCF production. Figure 5b indicates the variation percentage of fluorescence intensity with respect to a control culture (cells not treated with NC and not stimulated with H_2O_2). It can be seen that H_2O_2 produces a ~25% of ROS increment. ROS are efficiently scavenged by NC, and their values drop to a ~5% with respect to the basal levels in cells treated with 20 or 50 μg/ml of NC. No statistically significant scavenging effects are appreciable in cultures incubated with just 10 μg/ml. Most interestingly, NC induces a decrement of ROS basal levels even in cells not stimulated with H_2O_2. In this case, it can be again appreciated a slight, but significant, decrement of ROS production in cultures treated with 20 (~5%) and with 50 μg/ml of NC (~10%) with respect to the basal levels.

In order to investigate the mechanism of basal ROS decrement in NC-treated cells, qRT-PCR was carried out. Among the selected genes indicative of the redox status of the cells, a significant down-regulation of *Gss* and *Gpx1* induced by the 50 μg/ml NC 3-days treatment could be appreciated; *Gpx1* resulted down-regulated also by an incubation with 20 μg/ml NC; instead, no significant effects on *Txnrd1* were found at all the tested concentrations (Fig. 5c).

Effects of NC on Dopamine Production

ELISA test confirmed a production of dopamine following the 3-day incubation at all the tested NC concentrations. Dopamine amount, normalized to cell number, amounted to 2.5±2.3, 11.6±3.5, and 15.4±3.6 pg/ml/cell in the supernatants of PC12 cells treated with 0, 20, and 50 μg/ml of NC, respectively (Fig. 6a). These values indicate a strong effect of NC on dopamine secretion by the cells, with significant increase also at the lowest NC concentration tested (20 μg/ml).

At a gene level, a modulation induced by NC treatment for *Comt* and *Maoa* (1.5 fold increment at 50 μg/ml) could be noticed, while *Th* resulted unaffected (Fig. 6b). An interesting phenomenon of up-regulation in gene coding for protein involved in dopamine transport is highlighted: *Dat* transcription was 2 fold higher in cells treated with 20 μg/ml of NC, and about 3 fold higher for the 50 μg/ml dose (in both cases $p<0.05$); instead, *Vmat2* exhibited a 2 fold up-regulation after cell treatment with 50 μg/ml of NC (Fig. 6c).

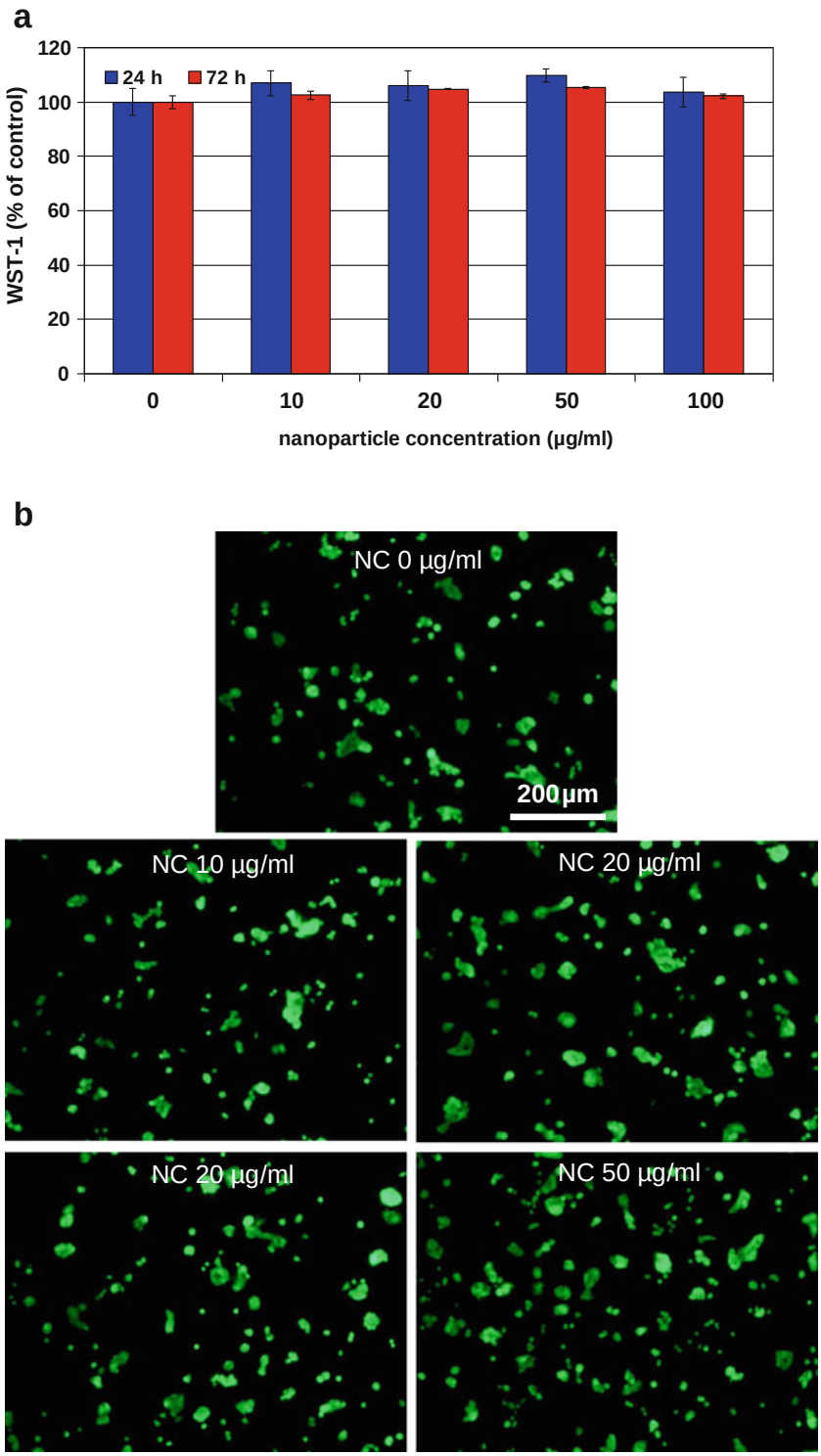

Fig. 2 WST-1 results at 24 and 72 h after incubation of PC12 cells with increasing concentrations of NC (**a**); Live/Dead® assay performed after 72 h (**b**).

DISCUSSION

Nanoceria holds great promises for the treatment of all those conditions where oxidative stress plays a key role. Impressive results have been already achieved: it is worth to mention the work by Rzigalinski and collaborators, that verified as NC behaves as an extremely efficient anti-ageing agent, increasing median lifespan in *Drosophila melanogaster* by 18 days (27).

Aiming at the exploitation of NC in the neurological field, here we have proposed a study of interactions of cerium oxide nanoparticles with PC12 cells. As already proven with many other cell lines, NC did not adversely affect viability and metabolic activity of PC12 cells, as

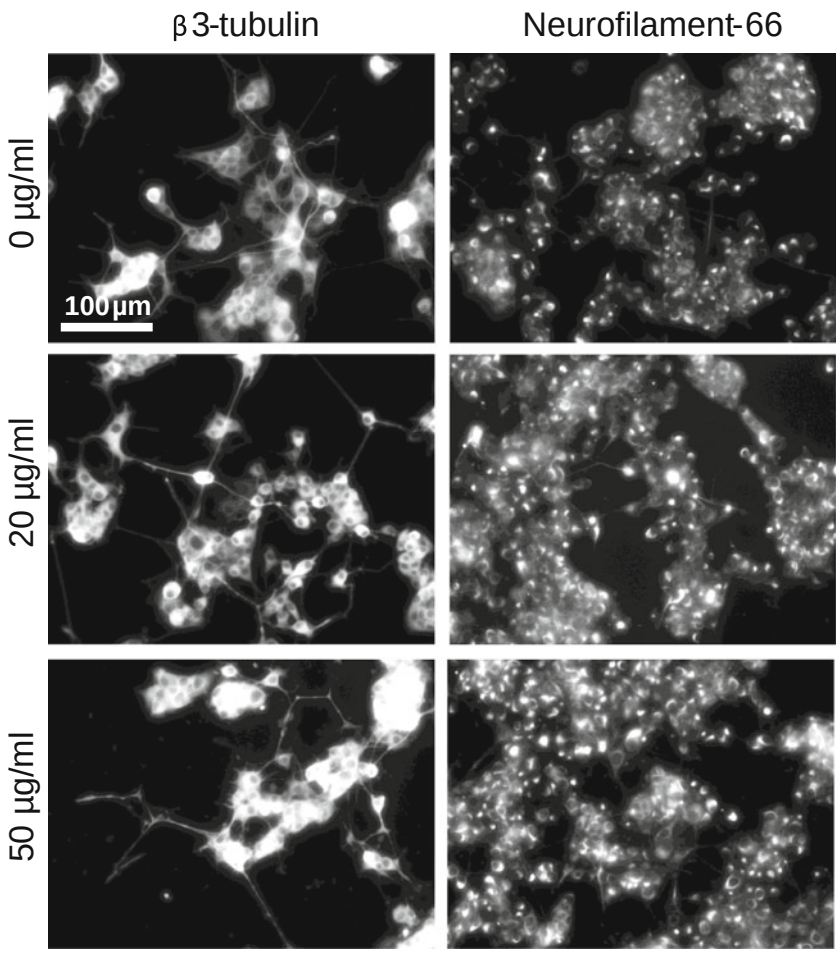

Fig. 3 Immunofluorescence staining of β3-tubulin and neurofilament-66 of PC12 cells differentiated for 3 days in the presence of increasing concentrations of NC.

demonstrated by both the Live/Dead® and the WST-1 assay, up to 100 μg/ml. Assessment of cytocompatibilty remains however a fundamental step before any other consideration; there are in fact, in the literature, some examples that show as NC could impair cell activities (28,29). These discrepancies can be explained by considering nanoparticle preparation procedure, nanoparticle size, internalization route, and cell line (30): it has been proven, in fact, as NC could be selectively toxic towards certain cancer cells, thus opening interesting perspectives also in cancer therapy (31). Nanoceria also did not impair neuronal differentiation of PC12 cells. Indeed, NC treated cells demonstrated a significant improved differentiation, in terms of a higher median neurite length (50% higher in cells treated with 50 μg/ml of NC) and of higher gene transcription of markers of neuronal differentiation, such as β3-tubulin and neurofilament-66. β3-tubulin is an early marker of neuronal differentiation (32), while neurofilament-66, also known as α-internexin, plays a key role in neurite outgrowth and regulates the expression of other neurofilaments (33), and was found to be expressed in cell somas and in the proximal segment of neurites.

Improvement of the differentiation process could be ascribable to a decrement of stress induced by ROS accumulation in the cells. As already proven for other cell models, NC is able to scavenge intracellular ROS also in PC12. A dose of 20 μg/ml was sufficient to reduce from 25% to 5% of the basal level ROS produced after H_2O_2 stimulation. Moreover, in cells not stimulated with H_2O_2, NC further reduces the basal levels of ROS up to 10% (at a dose of 50 μg/ml).

In order to investigate redox phenomena at gene level, qRT-PCR was carried out on genes coding for enzyme typically involved in ROS metabolism of PC12 cells (34). Three genes were selected: *Txnrd1*, *Gss* and *Gpx1*, which respectively encode thioredoxin reductase-1, glutathione synthetase, and glutathione peroxidase-1. The glutathione disulfide/glutathione pair (GSSG/GSH) and the thioredoxin reductase/thioredoxin system are in fact the major players in maintaining a favorable intracellular redox environment (35,36). After NC treatment, a down-regulation of *Gss* at 50 μg/ml and of *Gpx1* at both 20 and 50 μg/ml of NC concentration was noticed; on the contrary, no change in *Txnrd1* was detected. This result could be explained taking into account a mechanism of negative regulation by the cells: since NC acts as an exogenous anti-oxidant, natural

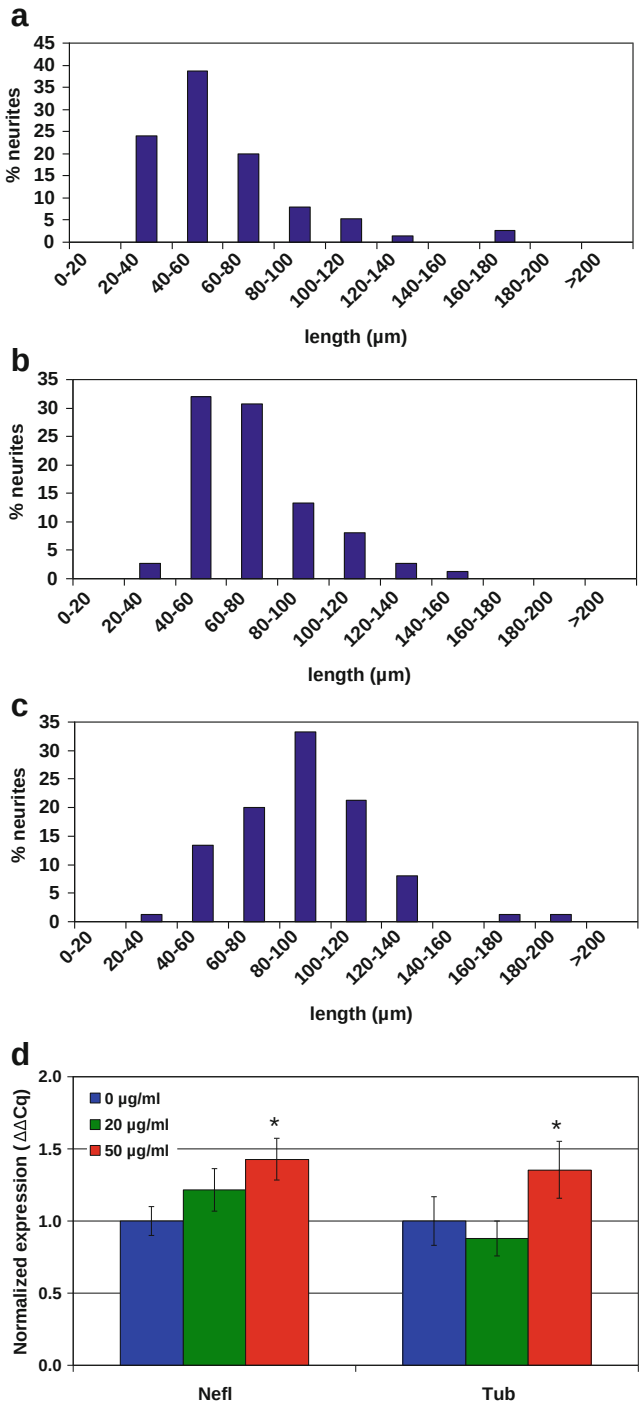

Fig. 4 Quantitative evaluation of PC12 differentiation: neurite length distribution of cells incubated in the presence of 0 (**a**), 20 (**b**) and 50 μg/ml (**c**) of NC; qRT-PCR results of β3-tubulin and neurofilament-66 gene transcription (**c**); * $p < 0.05$.

mechanisms of the cells are expressed in a lower extent, because of the presence of a further ROS scavenger represented by NC. The absence of oxidative stress even in a situation of *Gss*/*Gpx1* down-regulation is in fact confirmed by absence of significant alteration of *Txnrd1*, usually up-regulated following an oxidative insult (37). Nanoceria therefore acts in parallel to enzymes that usually scavenge ROS in cells. However, it should be carefully considered that it is also important to maintain a specific ROS level in cells. There are, in fact, some metabolic pathway were ROS play a relevant role in order to appropriately sustain cell activities, acting as useful signaling molecules that regulate physiological processes. This is the case, for example, of muscle tissue, where ROS have been shown to trigger many relevant signaling pathways (38). An accurate evaluation of NC effects on different cells and tissues is therefore mandatory, as well as a systematic consideration of the dose administered to the biological systems. If a systemic administration is envisioned, a specific functionalization of the nanoparticles should also be considered, in order to focus their ROS scavenger actions just on the desired cells/tissues, thus preventing potential side effects where, on the contrary, higher ROS levels are physiologically needed.

As previously pointed out, PC12 cells mimic many features of central dopaminergic neurons, including dopamine production. In evaluating whether the production of dopamine is affected by NC treatment, we highlighted an impressive, dose-dependent, increment of dopamine secretion by cells treated with nanoparticles, arriving at a 7-fold increment in cultures treated with 50 μg/ml of NC with respect to the controls.

In order to depict a better picture of NC effects on dopamine, we investigated transcription of *Th*, *Maoa*, and *Comt* genes, that are coding for tyrosine hydroxylase, monoamine oxidase A, and catechol-O-methyltransferase, respectively. Tyrosine hydroxylase is a key enzyme in dopamine synthesis, while monoamine oxidase A and catechol-O-methyltransferase are involved in dopamine metabolism (39). Nanoceria did not exhibit significant effects in *Th* trancription, but, at the highest tested concentration, an up-regulation of *Maoa* and *Comt* was found. An increased transcription of gene coding for enzyme involved in dopamine metabolism can be easily explained in view of a compensatory effect in cells induced by a higher dopamine content. The absence of a direct influence on *Th* suggests that beneficial effects of NC in dopamine production could be ascribable to its role in ROS depletion, rather than to a direct effect on the dopamine pathway.

The transcription of *Dat* and *Vmat2*, which encode for two transporters (dopamine transporter and vesicular monoamine transporter-2) was also affected by NC treatment. *Dat*, in particular, showed a 2-fold and a 3-fold transcription increment in cells respectively treated with 20 and 50 μg/ml of NC. Usually expressed at low levels in PC12 (39), dopamine transporter is a membrane protein involved in the re-uptake of dopamine, while vesicular monoamine transporter-2 is an integral membrane protein responsible of the transport of monoamines from cellular cytosol into synaptic vesicles. Once again, their up-

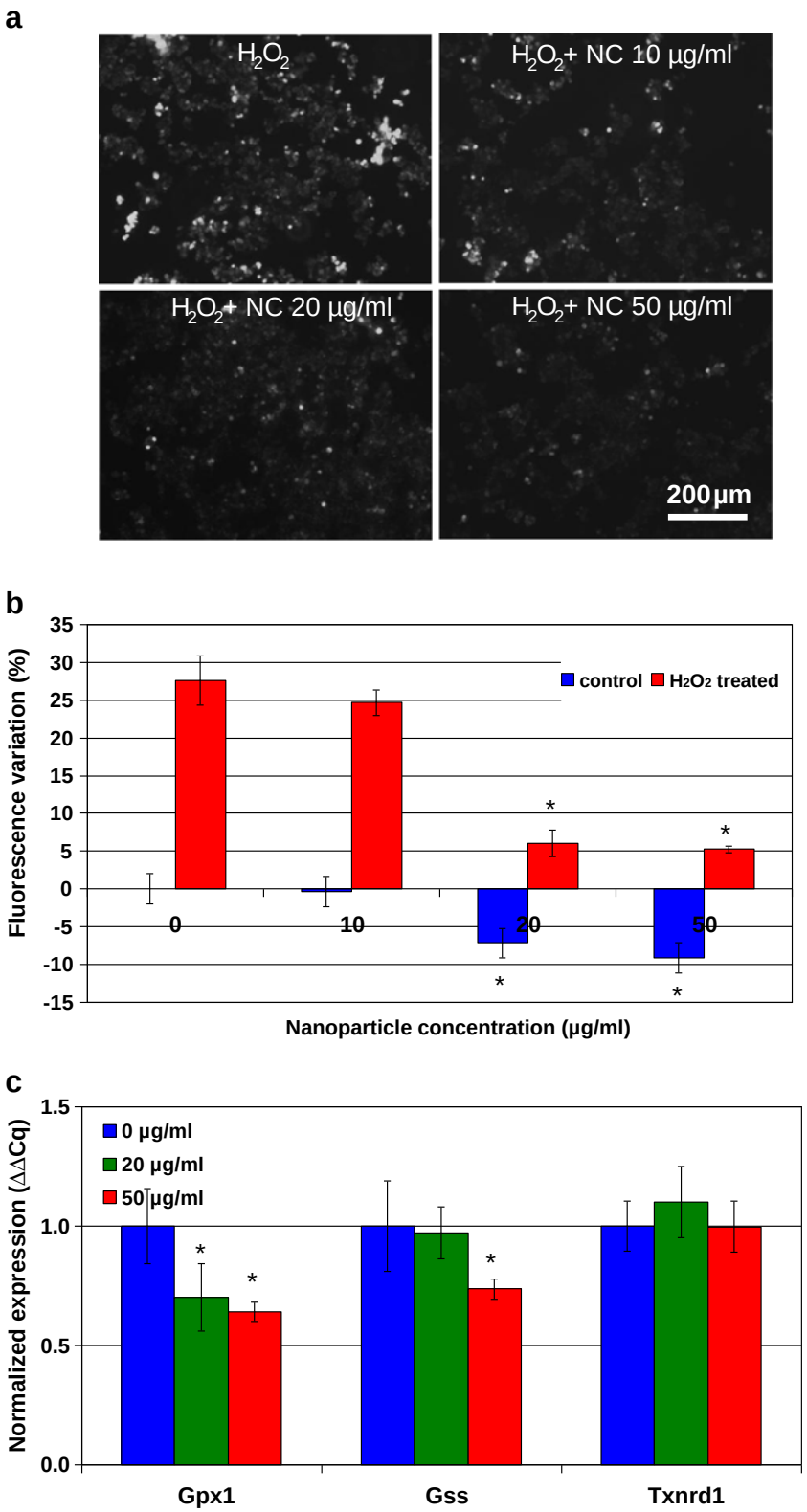

Fig. 5 Fluorescence ROS production detection in PC12 cells treated with increasing NC concentrations and, thereafter, stimulated with H_2O_2 50 μM (**a**); quantitative evaluation of ROS level in PC12 cells treated with increasing NC concentrations, with and without H_2O_2 stimulation (**b**); qRT-PCR evaluation of transcription of genes involved in cell redox mechanisms following NC treatment (**c**); * $p < 0.05$.

regulation is a consequence of a compensation mechanism due to an enhanced dopamine production by the cells.

Taken together, all the collected data indicate beneficial effects of NC on PC12 cells, both on neuronal differentiation and on dopamine production. These effects could be explained, in view of the performed analyses, on a more favorable intracellular environment due to lower ROS level, but direct effects on other

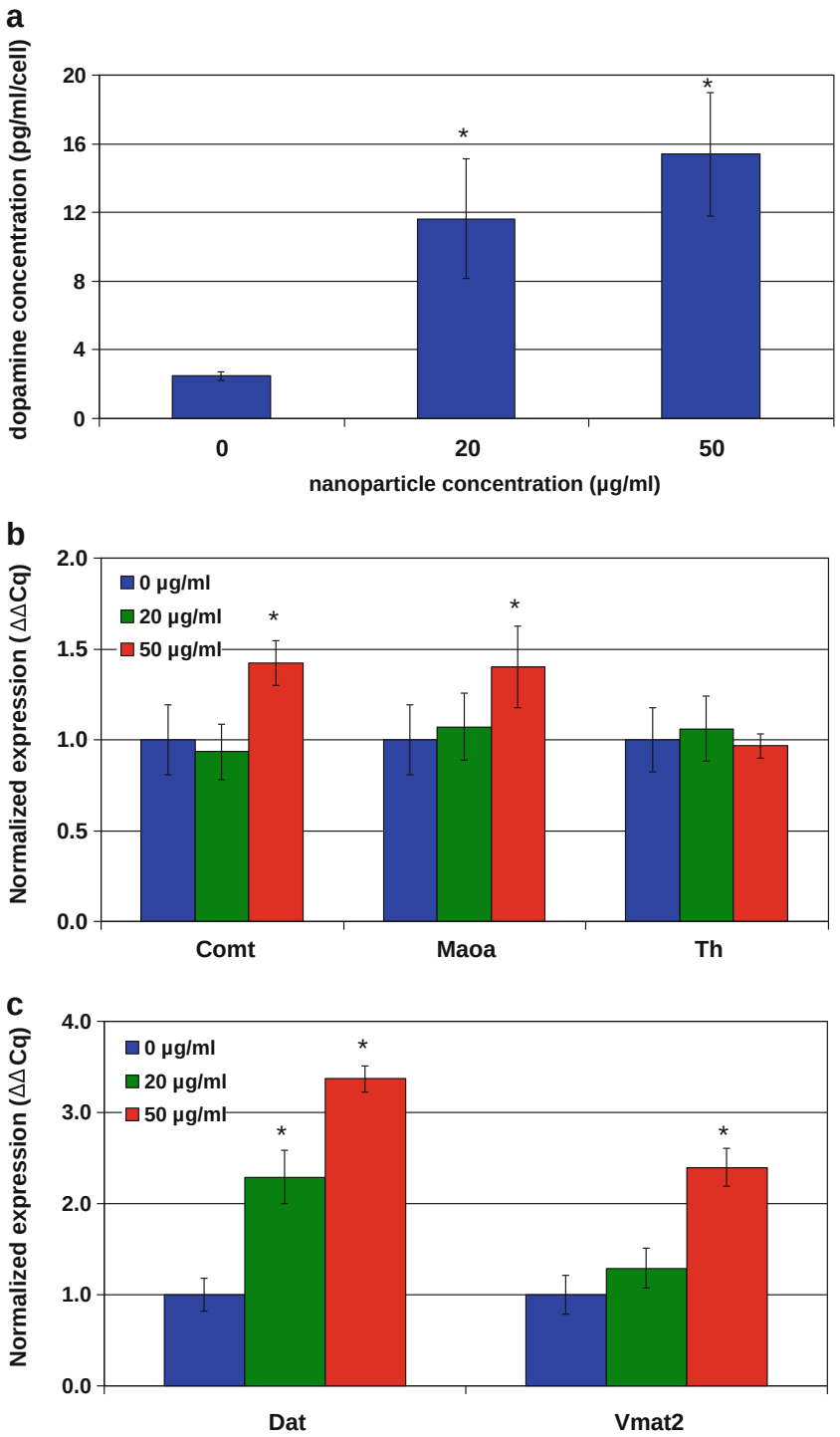

Fig. 6 Evaluation of dopamine production by PC12 cells treated with increasing NC concentrations (**b**); qRT-PCR evaluation of transcription of genes involved in dopamine metabolism (**b**) and transport following NC treatment (**c**); * $p < 0.05$.

metabolic pathway cannot be totally excluded. Future studies towards clinical translation will be devoted to the functionalization of cerium oxide nanoparticles in order to allow their targeting towards desired tissues, as well as their intracellular tracking. For *in vivo* neurological applications, the problem of blood brain barrier crossing will be addressed through functionalization with specific monoclonal antibodies (*i.e.*, Ox26 (40)). Furthermore, NC exploitation following other therapeutic approaches, like direct implantation of constructs aiming at replacing the function of impaired dopaminergic neurons, will be explored. This is the case, for example, of the transplant of encapsulated PC12 cells (41): NC could represent a promising physical cue to be integrated into polymeric scaffolds in order to improve dopamine secretion (42).

CONCLUSIONS

Applications of cerium oxide nanoparticles in the biomedical field have been exponentially grown during the latest years (43). Their impressive catalytic properties make this nanomaterial an extremely interesting inorganic antioxidant agent, that could find application against a huge number of pathological conditions (44). Our results on PC12 cells confirm the possibility of the exploitation of NC as a smart material for modulating cell metabolism and functions. Moreover, the highlighted increment of dopamine production following NC treatment highlights its high potential as countermeasure in neurodegenerative disorders. Of course, deeper examinations will be necessary in order to better clarify the mechanisms at the base of the documented effects; nonetheless, this study strongly encourages further investigations in this direction.

REFERENCES

1. Asati A, Lehmkuhl D, Diaz D, Perez JM. Nanoceria facilitates the synthesis of poly(o-phenylenediamine) with pH-tunable morphology, conductivity, and photoluminescent properties. Langmuir. 2012;28:13066–71.
2. Esposito V, Traversa E. Design of electroceramics for solid oxide fuel cell applications: playing with ceria. J Am Ceram Soc. 2008;91:1037–51.
3. Pirmohamed T, Dowding JM, Singh S, Wasserman B, Heckert E, Karakoti AS, et al. Nanoceria exhibit redox state-dependent catalase mimetic activity. Chem Commun. 2010;46:2736–8.
4. Heckert EG, Karakoti AS, Seal S, Self WT. The role of cerium redox state in the SOD mimetic activity of nanoceria. Biomaterials. 2008;29:2705–9.
5. Celardo I, Traversa E, Ghibelli L. Cerium oxide nanoparticles: a promise for applications in therapy. J Exp Ther Oncol. 2011;9:47–51.
6. Niu J, Wang K, Kolattukudy P. Cerium oxide nanoparticles inhibits oxidative stress and nuclear factor-κb activation in H9c2 cardiomyocytes exposed to cigarette smoke extract. J Pharmacol Exp Ther. 2011;338:53–61.
7. Schubert D, Dargusch R, Raitano J, Chan SW. Cerium and yttrium oxide nanoparticles are neuroprotective. Biochem Biophys Res Commun. 2006;342:86–91.
8. Pagliari F, Mandoli C, Forte G, Magnani E, Pagliari S, Nardone G, et al. Cerium oxide nanoparticles protect cardiac progenitor cells from oxidative stress. ACS Nano. 2012;6:3767–75.
9. Hirst SM, Karakoti A, Singh S, Self W, Tyler R, Seal S, et al. Biodistribution and in vivo antioxidant effects of cerium oxide nanoparticles in mice. Environ Toxicol. 2011. doi:10.1002/tox.20704.
10. Chen J, Patil S, Seal S, McGinnis JF. Rare earth nanoparticles prevent retinal degeneration induced by intracellular peroxides. Nat Nanotechnol. 2006;1:142–50.
11. Kong L, Cai X, Zhou X, Wong LL, Karakoti AS, Seal S, et al. Nanoceria extend photoreceptor cell lifespan in *tubby* mice by modulation of apoptosis/survival signaling pathways. Neurobiol Dis. 2011;42:514–23.
12. Zhou X, Wong LL, Karakoti AS, Seal S, McGinnis JF. Nanoceria inhibit the development and promote the regression of pathologic retinal neovascularization in the Vldlr knockout mouse. PLoS One. 2011;6:e16733.
13. Davan R, Prasad RGSV, Jakka VS, Aparna RSL, Phani AR, Jacob B, et al. Cerium oxide nanoparticles promotes wound healing activity in in-vivo animal model. J Bionanosci. 2012;6:78–83.
14. Celardo I, Pedersen JZ, Traversa E, Ghibelli L. Pharmacological potential of cerium oxide nanoparticles. Nanoscale. 2011;3:1411–20.
15. Reuter S, Gupta SC, Chaturvedi MM, Aggarwal BB. Oxidative stress, inflammation, and cancer: how are they linked? Free Radic Biol Med. 2010;49:1603–16.
16. Uttara B, Singh AV, Zamboni P, Mahajan RT. Oxidative stress and neurodegenerative diseases: a review of upstream and downstream antioxidant therapeutic options. Curr Neuropharmacol. 2009;7:65–74.
17. Bartsch H, Nair J. Chronic inflammation and oxidative stress in the genesis and perpetuation of cancer: role of lipid peroxidation, DNA damage, and repair. Langenbecks Arch Surg. 2006;391:499–510.
18. Kregel KC, Zhang HJ. An integrated view of oxidative stress in aging: basic mechanisms, functional effects, and pathological considerations. Am J Physiol Regul Integr Comp Physiol. 2007;292:18–36.
19. Janssen YM, Van Houten B, Borm PJ, Mossman BT. Cell and tissue responses to oxidative damage. Lab Invest. 1993;69:261–74.
20. Estevez AY, Erlichman JS. Cerium oxide nanoparticles for the treatment of neurological oxidative stress diseases. In: Oxidative stress: diagnostics, prevention, and therapy, ACS Symposium Series, 2011;1083:255–88.
21. Cimini A, D'Angelo B, Das S, Gentile R, Benedetti E, Singh V, et al. Antibody-conjugated PEGylated cerium oxide nanoparticles for specific targeting of Aβ aggregates modulate neuronal survival pathways. Acta Biomater. 2012;8:2056–67.
22. Estevez AY, Pritchard S, Harper K, Aston JW, Lynch A, Lucky JJ, et al. Neuroprotective mechanisms of cerium oxide nanoparticles in a mouse hippocampal brain slice model of ischemia. Free Radical Bio Med. 2011;51:1155–63.
23. Greene LA, Tischler AS. Establishment of a noradrenergic clonal line of rat adrenal pheochromocytoma cells which respond to nerve growth factor. Proc Natl Acad Sci USA. 1976;73:2424–8.
24. Le Bail A. Whole powder pattern decomposition methods and applications—A retrospection. Powder Diffr. 2005;20:316–26.
25. Romeo M, Bak K, El Fallah J, Lenormand F, Hilaire L. XPS study of the reduction of cerium dioxide. Surf Interface Anal. 1993;20:508–12.
26. Celardo I, De Nicola M, Mandoli C, Pedersen JZ, Traversa E, Ghibelli L. Ce^{3+} ions determine redox-dependent anti-apoptotic effect of cerium oxide nanoparticles. ACS Nano. 2011;5:4537–49.
27. Rzigalinski BA, Meehan K, Davis RM, Xu Y, Miles WC, Cohen CA. Radical nanomedicine. Nanomedicine UK. 2006;1:399–412.
28. Hussain S, Al-Nsour F, Rice AB, Marshburn J, Yingling B, Ji Z, et al. Cerium dioxide nanoparticles induce apoptosis and autophagy in human peripheral blood monocytes. ACS Nano. 2012;6:5820–9.
29. Tseng MT, Lu X, Duan X, Hardas SS, Sultana R, Wu P, et al. Alteration of hepatic structure and oxidative stress induced by intravenous nanoceria. Toxicol Appl Pharmacol. 2012;260:173–821.
30. Sohaebuddin SK, Thevenot PT, Baker D, Eaton JW, Tang L. Nanomaterial cytotoxicity is composition, size, and cell type dependent. Part Fibre Toxicol. 2010;7–22.
31. Asati A, Santra S, Kaittanis C, Perez JM. Surface-charge-dependent cell localization and cytotoxicity of cerium oxide nanoparticles. ACS Nano. 2010;4:5321–31.
32. Cooke MJ, Zahir T, Phillips SR, Shah DSH, Athey D, Lakey JH, et al. Neural differentiation regulated by biomimetic surfaces presenting

motifs of extracellular matrix proteins. J Biomed Mater Res A. 2010;93:824–32.
33. Chien CL, Liu TC, Ho CL, Lu KS. Overexpression of neuronal intermediate filament protein α-internexin in PC12 cells. J Neurosci Res. 2005;80:693–706.
34. Wang J, Rahman MF, Duhart HM, Newport GD, Patterson TA, Murdock RC, et al. Expression changes of dopaminergic system-related genes in PC12 cells induced by manganese, silver, or copper nanoparticles. Neurotoxicology. 2009;30:926–33.
35. Patenaude A, Murthy MR, Mirault ME. Emerging roles of thioredoxin cycle enzymes in the central nervous system. Cell Mol Life Sci. 2005;62:1063–80.
36. Maher P. Redox control of neural function: background, mechanisms, and significance. Antioxid Redox Signal. 2006;8:1941–70.
37. Yoo MS, Chun HS, Son JJ, DeGiorgio LA, Kim DJ, Peng C, et al. Oxidative stress regulated genes in nigral dopaminergic neuronal cells: correlation with the known pathology in Parkinson's disease. Brain Res Mol Brain Res. 2003;110:76–84.
38. Barbieri E, Sestili P. Reactive oxygen species in skeletal muscle signaling. J Signal Transduct. 2012;982794.
39. Fornai F, Lenzi P, Lazzeri G, Ferrucci M, Fulceri F, Giorgi FS, et al. Fine ultrastructure and biochemistry of PC12 cells: a comparative approach to understand neurotoxicity. Brain Res. 2007;1129:174–90.
40. Ulbrich K, Hekmatara T, Herbert E, Kreuter J. Transferrin- and transferrin-receptor-antibody-modified nanoparticles enable drug delivery across the blood–brain barrier (BBB). Eur J Pharm Biopharm. 2009;71:251–6.
41. Yoshida H, Date I, Shingo T, Fujiwara K, Kobayashi K, Miyoshi Y, et al. Stereotactic transplantation of a dopamine-producing capsule into the striatum for the treatment of Parkinson disease: a preclinical primate study. J Neurosurg. 2003;98:874–81.
42. Genchi GG, Ciofani G, Polini A, Liakos I, Iandolo D, Athanassiou A, et al. PC12 neuron-like cell response to electrospun poly (3-hydroxybutyrate) substrates. J Tissue Eng Regen M. 2012. doi:10.1002/term.1623.
43. Das S, Singh S, Dowding JM, Oommen S, Kumar A, Sayle TX, et al. The induction of angiogenesis by cerium oxide nanoparticles through the modulation of oxygen in intracellular environments. Biomaterials. 2012;33:7746–55.
44. Lord MS, Jung MS, Teoh WY, Gunawan C, Vassie JA, Amal R, et al. Cellular uptake and reactive oxygen species modulation of cerium oxide nanoparticles in human monocyte cell line U937. Biomaterials. 2012;33:7915–24.